Functions and biosynthesis of a tip-associated glycan in Streptomyces

Zhong, X.

4

5

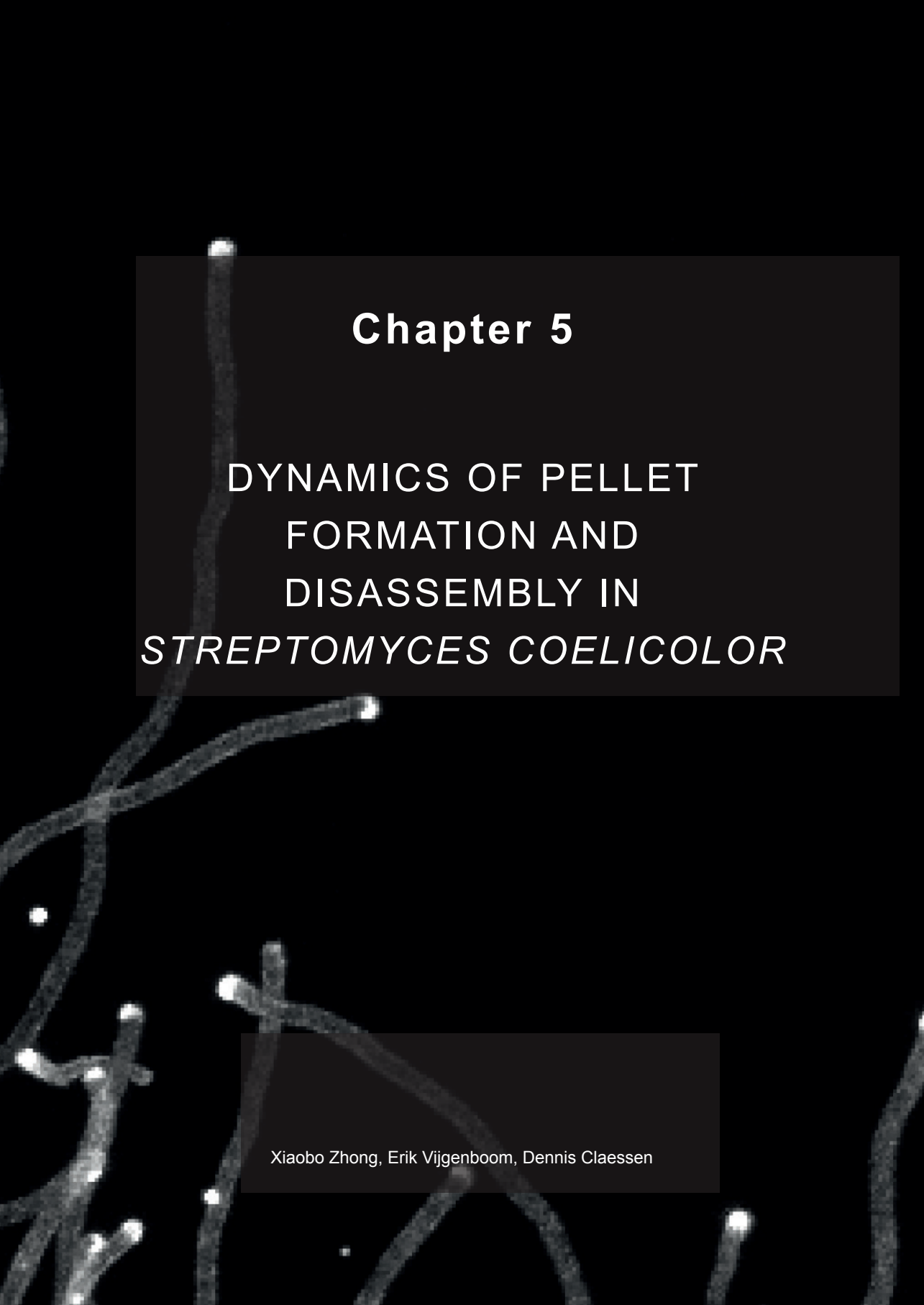

Chapter 5

DYNAMICS OF PELLET FORMATION AND DISASSEMBLY IN *STREPTOMYCES COELICOLOR*

Xiaobo Zhong, Erik Vijgenboom, Dennis Claessen

ABSTRACT

The similarities in genetic organization and phenotypic features of *S. coelicolor* M145 and *Streptomyces lividans* 66 have long been known. In liquid-grown environments, these two species produce large auto-aggregated biofilm-like structures, termed pellets. Aggregation in *S. lividans* strictly depends on a cellulose-like glycan, which is produced by the *cslA-glxA* operon. Here, we describe striking differences in pellet architecture of *S. lividans* 66 and *S. coelicolor* M145, the latter being fluffier throughout growth. Through fluorescent analyses we show that aggregation dynamics differ between both species, and that aggregation in *S. coelicolor* can occur in the absence of the cellulose-like glycan. We also show *cslZ,* which lies downstream of the *cslA-glxA* operon, is important for maintaining pellet integrity by ensuring proper deposition of the cellulose-like glycan. Altogether, our data gives a better understanding of pellet formation and disassembly in streptomycetes and hold promise for a better control over pellet morphology that is of interest for industrial application of these bacteria as production hosts.

Keywords: hydrolase, pellet fragmentation, biofilm, streptomyces

INTRODUCTION

Streptomycetes are well-known producers of bioactive molecules, including, but not limited to proteases, polysaccharide hydrolases and antibiotics (65, 154). Classically, *Streptomyces lividans* 66 and *S. coelicolor* M145 have been widely used for studying growth and morphogenesis in the streptomycetes. These two species have virtually identical (99.7%) 16S rDNA sequence and >90% of the proteins are either similar or identical (155, 156). Despite the high similarity in these two species, there are some striking differences. For instance, contrary to *S. coelicolor*, *S. lividans* lacks a methylation-dependent restriction system, which makes *S. lividans* more suitable as a host for DNA cloning (157). In addition, *S. lividans* has very low endogenous extracellular proteolytic activity (158), which is suitable for higher enzyme production on industry. From this perspective, morphogenesis of liquid-grown streptomycetes was well-studied in *S. lividans*, while little is known in *S. coelicolor*. On the other hand, genetic differences in these two species are also reflected in metabolic differences, wherein oxidative metabolism predominates in *S. coelicolor* and correlates with the production of blue-pigmented antibiotic actinorhodin, whereas the metabolism of *S. lividans* was proposed to be mainly glycolytic (159).

Streptomycetes form filamentous networks of interconnected hyphae, called mycelia. Many species form so-called pellets in liquid environments, which are auto-aggregated assemblies of mycelia. In *S. lividans,* pellets form by the assembly of germlings and small mycelial fragments into larger structures (25, 26). Following growth and further densification, pellets are obtained that for some species can be close to 1 mm in size. Eventually, ageing pellets will release mycelial fragments into the environment in a process termed fragmentation. When sufficient nutrients are available, such fragments can reinstate growth and establish new pellets (26).

Morphogenesis of *Streptomyces* pellets depends on the interplay between environmental and genetic factors. For instance, morphology is strongly affected by specific growth conditions, such as the stirring speed, pH and osmolyte concentrations (23). Besides environmental factors, morphology of pellets is also dictated by genetic factors. Formation of pellets in *Streptomyces* depends on the presence of two surface polysaccharides, poly-β-(1,6)-N-acetylglucosamine (PNAG) (48) and a cellulose-like glycan (5). The PNAG polymer is synthesized by the mycelial aggregation-related genes *matA* and *matB*, which promote hypha-hypha interactions and which are

sufficient to induce pellet formation in non-pelleting strains (48, 49). Deletion of *matA* and *matB* causes very small and open mycelia, respectively. Likewise, mycelia also grow with an open structure when the cellulose-like glycan is absent (27). Our previous studies indicated that the PNAG polymer and the cellulose-like glycan contribute to the aggregation of germlings at the early stage of pellet formation in *S. lividans* (25).

The cellulose-like glycan in *S. coelicolor* is synthesized by a gene cluster putatively ranging from SCO2833-SCO2838, in which SCO2836 and SCO2837 encode the cellulose synthase-like protein CslA and the radical copper oxidase GlxA, respectively. SCO2833 encodes the recently characterized lytic polysaccharide monooxygenase LpmP, while SCO2838 encodes glucanase CslZ (14). CslA and GlxA are responsible for synthesis of the cellulose-like glycan and the absence of either gene results in a non-pelleting phenotype, which is also observed when both *lpmP* and *cslZ* are absent (14, 27). LpmP and CslZ are thought to cooperatively facilitate deposition of the cellulose-like glycan at the cell surface by creating a passage through the peptidoglycan layer (14). Deletion of either *cslZ* or *lpmP* reduced deposition of the glycan but had no major effect on pellet formation. How deranged synthesis and deposition of the glycan affects later stages of morphogenesis and fragmentation is unknown.

In this study, we performed a comprehensive analysis of CslZ functioning related to pellet morphogenesis in *S. coelicolor*. The absence of *cslZ* dramatically reduced glycan deposition at hyphal tips, which not only inhibits mycelial aggregation, but also promotes pellet fragmentation. In addition, we show that the dynamics in pellet formation and disassembly differ between *S. coelicolor* and *S. lividans.* Taken together, these results better our understanding of mycelial morphogenesis in liquid environments.

MATERIALS AND METHODS

Bacterial strains and growth conditions

All strains used in this study are listed in Table S1. *E. coli* DH5α and *ET*12567 harbouring pUZ8002 were used to construct and obtain non-methylated plasmids, respectively. All *E. coli* strains were grown at 37 °C in LB medium with appropriate antibiotics, if necessary.

For the collection of spores and conjugation, *Streptomyces* strains were grown on Mannitol Soy Flour (MS) solid medium (160). To study pellet morphogenesis and

actinorhodin production, spores were inoculated into 100 ml TSBS medium (160) at a final concentration of 10^6 CFUs ml^{-1} and grown at 30 °C in unbaffled Erlenmeyer flasks equipped with metal coils.

To study aggregation between germlings of *S. coelicolor*, spores of fluorescent derivative strains ($5x10^5$ CFUs ml^{-1}) were mixed in fresh TSBS medium in a 1:1 ratio and grown for 16 hours. Mycelium aggregation was studied by growing the fluorescent strains separately for 16 hours (in 50 ml cultures), followed by washing and mixing them in a 1:1 ratio into 100 ml fresh medium. Cultures were then grown for another 8 hours before imaging.

Primers, plasmids construction and transformation

Primers and plasmids used in this study are shown in Table S2 and Table S3, respectively. To introduce new plasmids into a previously constructed apramycin-resistant *cslZ* mutant (35), the apramycin cassette was removed using the Cre-Lox recombinase system (161), thereby generating a marker-less *cslZ* mutant.

To make fluorescent derivative strains constitutively expressing eGFP or mCherry, the sequences encoding these proteins were amplified from plasmids pGreen and pRed (162) using the GFP-F/GFP-R primers (Table 2). The amplified fragments were cloned into pXZ3 (14), which contains *lpmP* expressed from the *gapAp* promoter, using NdeI and BamHI restriction enzyme sites. In this way, the *lpmP* coding sequence was replaced by *eGFP* or *mCherry*, yielding pXZ37 and pXZ38, respectively.

To make green and red fluorescent strains constitutively expressing *cslZ*, the pXZ37 and pXZ38 plasmids were digested with XbaI and BamHI followed by isolation of the *gapAp-eGFP* and *gapAp-mCherry* fragments. These fragments were subsequently cloned into XbaI/BamHI digested pXZ2 plasmid (14), yielding pXZ39 and pXZ40 respectively. Finally, these plasmids were introduced into the *S. coelicolor* strains by conjugation (87).

Sedimentation assay

To qualitatively assess fragmentation, a sedimentation assay was used. Briefly, 5 ml of 24, 48and 72h-old cultures were transferred to 10 ml glass tubes. Sedimentation in the tubes was imaged after 90 minutes in standing state.

Quantification of fragments and biomass in liquid-grown cultures

Quantification of fragments was performed essentially as described (26). Briefly, 10^6 CFU ml^{-1} of fresh spores were inoculated into 100 ml TSBS medium. At each time point (24, 48 and 72 h), 5 ml of cultures were taken and sequentially filtered through 100, 40, and 5 µm strainers (Falcon®). The final filtration was diluted with Milli-Q water and plated on MS agar plates. After growth of 72h at 30 °C, the Colony Forming Units (CFUs) were counted.

Dry weight measurements were used to quantify biomass production. To this end, 2 ml samples were obtained from the cultures, washed twice with Milli-Q water and dried overnight at 30 °C. All measurements were done in triplicate and blanked against dried empty tubes.

Microscopy

Imaging of pellets was done using a Zeiss Axio microscope equipped with an Axiocam 105 camera. Fluorescent microscopy was done using a a Zeiss LSM900 Airyscan 2 microscope.

For imaging of β-(1-4) glycans, mycelium was stained with calcofluor white (Sigma) and analysed as before (14). For visualization of aggregation, whole slide imaging was performed using a region of 6x6 tiles. All images were processed using ImageJ software (version 2.0.0/1.53c/Java 1.8.0_172/64-bit) (163).

RNA isolation and RT-qPCR

Total RNA was isolated from cultures grown for 16, 24, 32, 40 and 48 hours in TSBS medium using modified Kirby mix and phenol/chloroform extraction, followed by treatment with RNase free-DNase I as described (87). Following RNA isolation, 2 µg RNA from each strain was used to generate cDNA with iScriptTM Advanced cDNA synthesis kit (Bio-Rad). Then, RT-PCR reaction products were diluted 10-fold and 1 µl was used for a quantitative PCR with universal SYBR® Green Supermix (Bio-Rad) according to instructions of the manufacturer. The house-keeping gene *16S rRNA* (164) and the gene *hrdB* (SCO5820), which encodes the major vegetative sigma factor of *S. coelicolor* and expressed at relatively constant level throughout growth (165), were used as internal controls. Quantitative PCR was performed by CFX96

Touch Real-Time PCR Detection System (Bio-Rad) and data was processed by CFX Manager software (Bio-Rad, version 3.1), in which the transcription of *cslZ* and *cslA* relative to the internal controls was calculated by the relative quantitative $2^{-\Delta\Delta Cq}$ method (166). All primers used in the qPCR reactions are listed in Table 2.

Actinorhodin quantification

Quantification of actinorhodin (ACT) production is performed as described (167) with following modifications. After growing strains in TSBS medium for 72 h, pellets were removed by the centrifuge (3000 *g* for 5 min). 1.25 ml of cultural supernatant was collected and supplemented with 0.25 ml 3M HCl. After an overnight incubation at 4 °C, precipitated ACT was collected (13,000 *g* for 30 min) and resuspended in 250 µl 1M KOH. Absorbance at the wavelength of 640 nm of samples was blanked against 1M KOH and used to evaluate the quantification of ACT. All measurements were done in triplicate.

RESULTS

Pellet architecture comparison between *S. coelicolor* and *S. lividans*

Formation of pellets has been mostly studied in *S. lividans,* which is the industrial workhorse for production and secretion of proteins (25, 26). Despite its close relationship, the pellets of *S. coelicolor* in liquid culture appear quite different from those of *S. lividans* (Fig. 1). More specifically, those of *S. coelicolor* have a relative fluffy appearance due to the protrusion of hyphae from the pellet surface. This prompted us to investigate if this coincided with an increase of detached fragments in the culture broth. To this end, we transferred 2 ml of a seed culture of *S. coelicolor* M145 or *S. lividans* 66, which had been growing for 24, 32 or 48 hours, into 100 ml fresh TSBS medium and allowed these subcultures to grow for another 24 hours. In this way, detached fragments in the seed culture would be able to outgrow into new (small) pellets and thus causes morphological heterogeneity (26). Notably, the pellets of *S. lividans* were homogenous in size when 24 or 32-h-old seed cultures were used, indicating that little fragmentation had occurred. In contrast, the pellets of *S. coelicolor* appeared highly heterogenous in size and shape regardless of the seed culture age (Fig. 1). These results demonstrate that the increased fluffiness of *S. coelicolor* pellets leads to more fragmentation and mycelial heterogeneity.

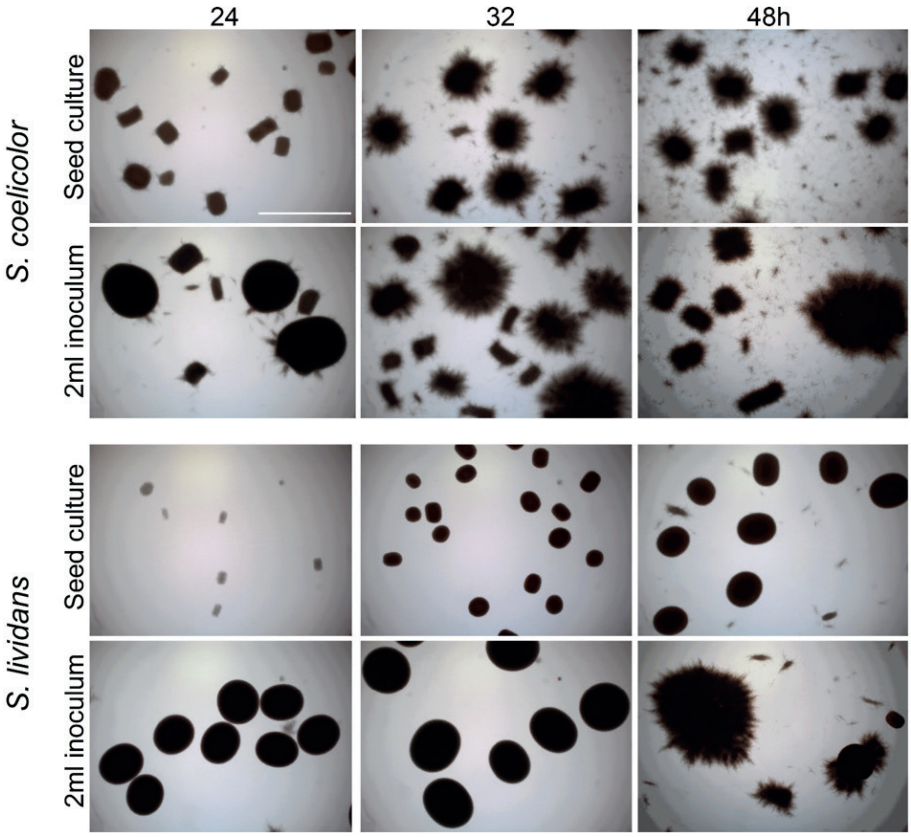

Figure 1 Morphological comparison between pellets of *Streptomyces lividans* and *S. coelicolor*. Seed cultures (**Top panel**) were obtained by inoculating 10^6 CFU ml^{-1} spores in 100 ml TSBS medium followed by growth for 24, 48 and 72 h. 2 ml of these seed cultures were used to inoculate fresh TSBS cultures followed by growth for another 24 h. Please note the homogeneity of the *S. lividans* cultures compared to *S. coelicolor*, particularly after 24 and 32 hours. The scale bar represents 50 µm.

CslZ is involved in aggregation of clumps in *S. coelicolor*

We previously showed that aggregation between germlings and mycelia in *S. lividans* is governed by the CslA-dependent glycan. To study the role of CslA, but also CslZ in aggregation in *S. coelicolor*, we created a series of fluorescent reporter strains. More specifically, we constructed red- and green-fluorescent derivatives of an apramycin resistant wild-type strain, a Δ*cslA* mutant, a Δ*cslZ* mutant and a strain constitutively expressing *cslZ* from the *gapAp* promoter. When spores of strains expressing *eGFP* or *mCherry* were mixed at the onset of growth, all pellets were composed of both types of

fluorescent hyphae, independent of the genetic background (Fig. S1). This is in stark contrast to *S. lividans*, where aggregation between germlings was dependent on the presence of CslA (25). However, we did observe a strong defect in aggregation when the fluorescent strains were cultured separately for 16 hours and then mixed (Fig. 2). More specifically, whereas 14% of the wild-type pellets were composed of red and green hyphae, only 7.5% were so in the strain lacking *cslZ*. Reversely, constitutive expression of *cslZ* yielded pellets that were in 63.6% composed of red- and green-fluorescent hyphae (Fig. 2). Altogether, these results reveal that CslZ is important for aggregation of mycelial clumps. Furthermore, they show that aggregation in *S. coelicolor* can occur in a CslA-independent manner.

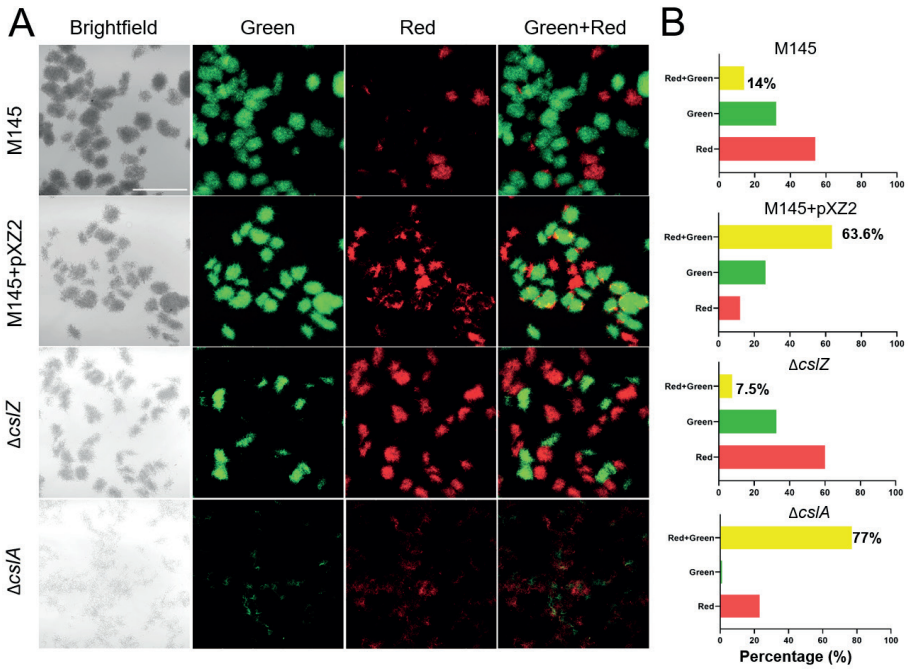

Figure 2 Aggregation of mycelial clumps depends on *cslZ* in *S. coelicolor*. (**A**) Representative images in co-cultures of red- and green-fluorescent derivatives of the wild-type strain, the Δ*cslZ* mutant and strains constitutively expressing *cslZ* (M145+pXZ2). Co-cultures were obtained by mixing the fluorescent strains, which had been grown separately for 16 h, and then allowing them to grow for another 4 hours. The scale bar represents 100 µm. (**B**) Quantification of fluorescent pellets as quantified using whole slides imaging (168). Fluorescent pellets were counted manually and graphs were generated by GraphPad Prism software (version 8.0.2).

Reduced glycan deposition correlates with increased fragmentation

We previously showed that the absence of the CslA-dependent glycan led to an open mycelial structure for *S. coelicolor*. Meanwhile, the absence of *cslZ* affects deposition of the glycan in 16 h-old cultures, but had no dramatic effect on pellet formation (14, 28). To investigate how the disturbed and reduced deposition of the glycan relates to fragmentation, we performed a sedimentation assay and quantified the number of fragments. The M145 strain containing the empty plasmid pSET152 (pM145) was used as a control. Quantitative analysis indicated that the number of fragments in the culture of the Δ*cslZ* mutant was approximately 3-4 times higher in comparison to the wild-type strain or the strain carrying the empty plasmid pSET152, in particular after 48 and 72 hours of growth. The larger number of fragments also led to a higher growth speed of the Δ*cslZ* mutant, as concluded from the higher amount of biomass in the culture (Fig. 3A, Fig.3B). By contrast, when *cslZ* was expressed constitutively from the *gapAp* promoter, the number of fragments was dramatically reduced (Fig. 3B). This strain had 20 times less fragments at 48 hours in the medium and grew poorly compared to the wild-type and control strains. These effects on mycelial growth were confirmed by the sedimentation assay where the Δ*cslZ* mutant settled more pellets than the wild-type and the control strain in 90 min, while constitutively expression of *cslZ* dramatically inhibited the production of pellets within the same time (Fig. 3C). These data show that the absence and overproduction of *cslZ* correspondingly promotes and inhibits fragmentation.

Quantitative analysis of the cellulose-like glycan indicated that, in comparison to the wild-type strain, increased fragmentation of the Δ *cslZ* mutant correlates with reduced CFW staining at hyphal tips, while reduced fragmentation of *cslZ* constitutively expressed strain with increased staining at hyphal tips (Fig. 4A, Fig. 4B). These results indicate that CslZ affects pellet fragmentation at the level of the CslA-dependent glycan. To further corroborate the relationship between *cslZ* and *cslA*, we analyzed their expression patterns with quantitative PCR at different time points during pellet development. The analysis showed that both genes follow a similar expression pattern (Fig. 4C). Furthermore, expression of both genes is high in the younger cultures but decreases after 16 hours of growth (Fig. 4C). Strikingly, the expression pattern is consistent with the detection of the cellulose-like glycan at hyphal tips (Fig. 4C). Altogether, these results show that CslZ is required for glycan deposition, which in turn reduces fragmentation.

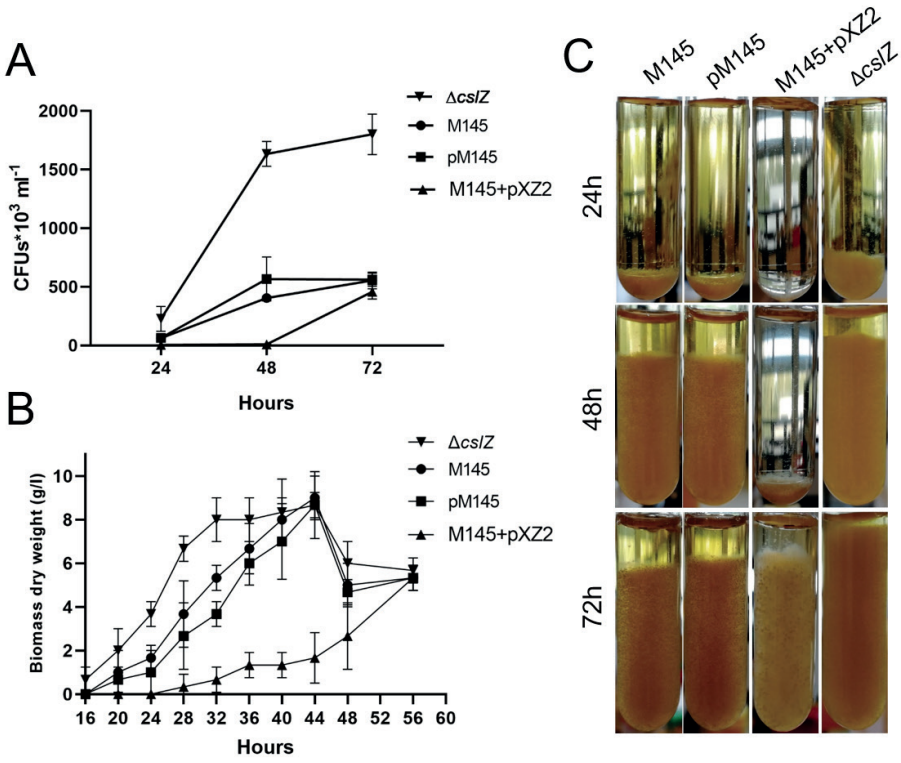

Figure 3 The absence of CslZ affects pellet morphology in *S. coelicolor*. (**A**) Fragments were obtained by the sequential filtering of TSBS cultures which had been grown for 24, 48 or 72h through cell strainers with a pore size of 100, 40 and 5 µm. Fragments were quantified by their ability to grow out into Colony Forming Units (CFUs). (**B**) Dry weight measurements of *S. coelicolor* strains over time. All measurements were performed in triplication. Error bars represent the standard error of the mean. (**C**) Sedimentation assays. The wild-type strain (M145), the Δ*cslZ* mutant and the strain constitutively expressing *cslZ* (M145+pXZ2) were grown in TSBS medium. M145 carrying the empty pSET152 plasmid was used as a control. For each strain, 5 ml of 24, 48, 72h-old cultures were transferred into glass tubes and pictures were taken after 90 minutes of sedimentation.

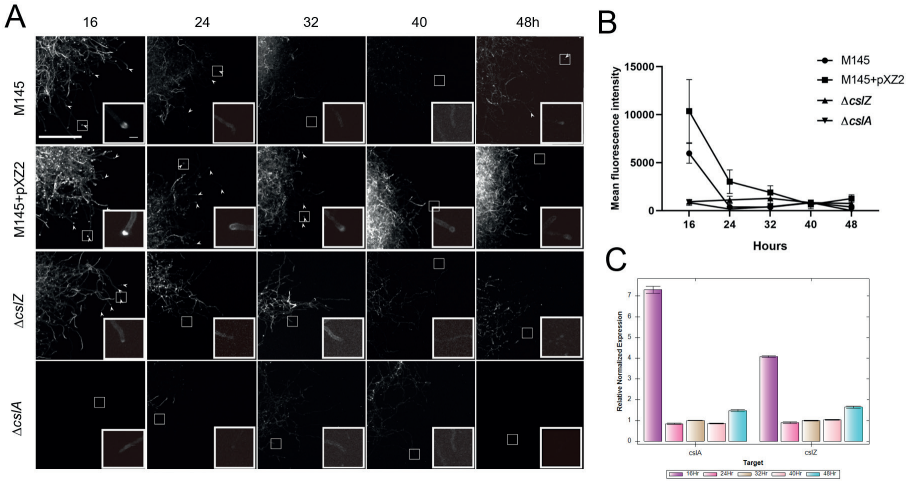

Figure 4 *cslZ* is involved in deposition of *cslA*-dependent glycan. A Calcofluor white (CFW) staining was used to detect β-(1,4)-glycans in *S. coelicolor* strains lacking or overexpressing *cslZ*. The Δ*cslA* mutant was used as control. Images were taken at time points of 16, 24, 32, 40, 48 h. Representative CFW stained tips are indicated with arrowheads. Scale bar represents 200 µm (main images) and 1µm (insets). **B** The mean fluorescence intensity of calcofluor white-stained tips was determined for 20 tips in each strain. The fluorescence intensity at every hyphal tip was measured in square regions of 1.5 µm x 1.5 µm and corrected for the background fluorescence. Error bars represent the standard error of the mean. **C** Quantitative analysis of *cslZ* expression in 16, 24, 32, 40, 48 h-old liquid grown *S. coelicolor* cultures. The *hrdB* gene (SCO5820) and *16S rRNA* were used as reference genes. The bar graph was generated using CFX Manager software. Error bars represent the standard error of the mean.

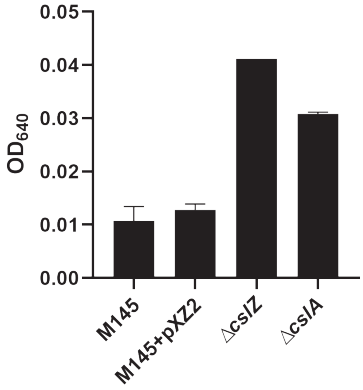

Figure 5 Detection of actinorhodin production. Strains were grown in TSBS medium for 72 h at 30 °C, 1.25 ml of cultural supernatant was collected after removing pellets. Then, 0.25 ml 3M HCl was added to precipitate ACT, which was subsequently resuspended in 0.25 ml 1M KOH and the OD_{640} was measured. Bars represent standard errors of the mean.

The absence of *cslZ* promotes actinorhodin production

Actinorhodin (ACT) is a typical antibiotic produced by *S. coelicolor*. Production of ACT requires a minimal mycelial pellet size (169). All our results demonstrated that deletion of *cslZ* promotes mycelial heterogeneity of *S. coelicolor*. To test if the pellet morphology changes in the absence of *cslZ* affects ACT production, we compared the Δ*cslZ* mutant and wild-type strain grown in TSBS medium. The Δ*cslA* mutant and a strain constitutively expressing *cslZ* were used as controls. Fig. 5 shows, in comparison with the wild-type strain, the Δ*cslZ* mutant and Δ*cslA* mutant produces 4 and 3 times higher of ACT, respectively. The strain constitutive expression of *cslZ* has no obvious change on ACT production. These results indicate that promotion of pellet fragmentation by the deletion of *cslZ* enhance actinorhodin production.

DISCUSSION

Streptomycetes are an important source for enzymes and antibiotics, and their morphogenesis in submerged environments has been an emerging topic over the past years (170). *S. lividans* 66 is the best studied species for pellet morphology, for which cell surface-associated glycans are required. Pellet formation in *S. lividans* depends on the aggregation of germlings and mycelial clumps, both of which depend on the cellulose-like glycan and the MatAB-dependent PNAG polymer (26, 48). As the model organisms of *Streptomyces* genus, *S. lividans* 66 and *S. coelicolor* M145 are very closely related and seem to follow the same development mode. However, analysis with fluorescent reporters demonstrated that aggregation of germlings in *S. coelicolor* occurs independently of the cellulose-like glycan (Fig. 4, Fig. S1), while the cellulose-like glycan is important for aggregation of mycelial clumps in *S. coelicolor* (Fig. 4). Altogether, this demonstrates that germling aggregation in *S. coelicolor* can occur in a CslA-independent manner, in which large amounts of PNAG polymer produced at early timepoints may paly such roles instead. Indeed, constitutive expression of *matAB* form *gapAp* promoter are sufficient to induce pellet formation in non-pelleting strains.

Our work also shows that fragmentation in *S. coelicolor* and *S. lividans* occur at different stages of growth. Fragmentation in S. *lividans* 66 coincides with the cultures entering stationary phase (26). In contrast, fragmentation of *S. coelicolor* appears to occur independent of the culture age and is already observed at time points when the medium is not exhausted for nutrients. Notably, pellets of *S. coelicolor* appear fluffier than those of *S. lividans* (see Fig. 1). This provides a plausible explanation for the

increased fragmentation, given that the protruding hyphae can easily detach from the edge of pellets by shear stress, which can subsequent grow out to form new pellets. This in turn dramatically increases culture heterogeneity. Why more filaments protrude from the cell surface is unknown, but this may reflect differences in macromolecules, such as, amongst others, the glycans mediating adhesion.

Fragmentation is a crucial part of the life cycle of pellets. Fragmentation is affected by many external factors in bioreactors, such as, but not limited to pH, shear stress and concentration of osmolytes (171, 172). However, analysis of pellet fragmentation in streptomycetes at the genetic level had not studied before. Here, we show that the absence of *cslZ* facilitates fragmentation by decreasing the amount of surface located cellulose-like glycan at hyphal tips. In many streptomycetes, *cslZ* is adjacent to the *cslA-glxA* operon (14). Combining the results of glycan quantification and quantitative PCR (Fig. 4), we demonstrated that CslZ is essential for proper deposition of the cellulose-like glycan. On the other hand, we noticed that, at 72h, the strain constitutively expressing *cslZ* appeared to switch morphology from dense pellets to the release of numerous mycelial fragments (Fig. 3A, Fig. 3C). Given that the glucanase CslZ is a promiscuous hydrolase (14), we think it may also target the cellulose-like glycan. Lysis of hyphae in older cultures may release CslZ from the membrane fraction. Indeed, preliminary data show that CslZ is present in spent medium after 72 hours in the strain constitutively expressing CslZ (our unpublished data). CslZ may thus play two distinct roles: it may first help to create pellets, while in older cultures help to promote fragmentation.

The dynamic process of pellet formation and fragmentation is of interest for the application of streptomyces as a host in industrial production processes. Therefore, it is essential to elucidate all players involved in pellet morphology to gain control over mycelial heterogeneity, which may adversely affect productivity (23, 173). In addition, the unique morphogenesis of *Streptomyces* in liquid environments has striking similarities with biofilm development of other microbes including pathogens (26), Therefore, exploring pellet development in further detail could contribute to a better understanding of biofilm development.

SUPPLEMENTAL DATA

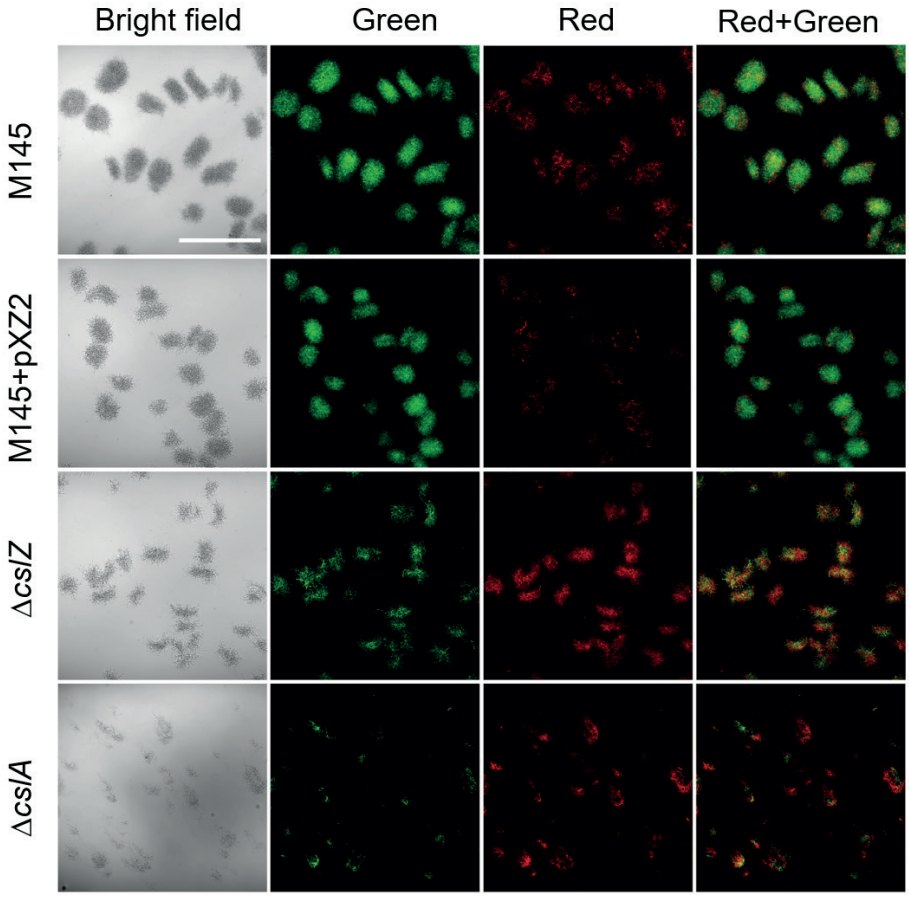

Supplementary Figure 1. Aggregation of germlings in *S. coelicolor* does not depend on CslA or CslZ. 5x10^5 CFUs ml^{-1} of green- and red-fluorescent derivatives of the wild-type strain, the Δ*cslZ* mutant and the strain constitutively expressing *cslZ* (M145+pXZ2) were mixed and inoculated into 100 ml TSBS medium. Images were taken after 16 h of growth at 30 °C. Scare bar represents 200 µm.

Supplementary Table 1. Strains used in this study

Bacterial Strains	Description	References
E. coli		
DH5α	F- Φ80lacZDM15, Δ(lacZYA-argF), for cloning	Laboratory collection
ET12567(PUZ8002)	dam- dcm- hsdS, RP4 transfer gene	Laboratory collection
Streptomyces		
M145	Wild-type *Streptomyces coelicolor* A3(2) strain	Laboratory collection
S. lividans 66	Wild-type *Streptomyces lividans* strain	Laboratory collection
pM145	M145 containing empty pSET 152 plasmid :: *aac(3)IV*	(14)
M145+pXZ2	*S. coelicolor* M145 containing pXZ2 that constitutively expresses *cslZ* from *gapAp* promoter	(14)
Δ*cslA*	M145 lacking *cslA* gene (SCO2836) :: marker-less	(48)
Δ*cslZ*	M145 lacking *cslZ* gene (SCO2838) :: marker-less	This work
M145+pXZ2f	*S. coelicolor* M145 containing pXZ2f that constitutively expresses *cslZ-flag* fragment from *gapAp* promoter	(14)
M145+ pXZ37	*S. coelicolor* M145 containing pXZ37 that constitutively expresses *eGFP* from *gapAp* promoter	This work
M145+ pXZ38	*S. coelicolor* M145 containing pXZ38 that constitutively expresses *mCherry* from *gapAp* promoter	This work
Δ*cslZ*+ pXZF1	*cslZ* mutant containing pXZF1 that constitutively expresses *eGFP* from *gapAp* promoter	This work
Δ*cslZ*+ pXZF2	*cslZ* mutant M145 containing pXZF2 that constitutively expresses *mCherry* from *gapAp* promoter	This work
Δ*cslA*+ pXZ37	*cslA* mutant containing pXZ37 that constitutively expresses *eGFP* from *gapAp* promoter	This work
Δ*cslA*+ pXZ38	*cslA* mutant M145 containing pXZ38 that constitutively expresses *mCherry* from *gapAp* promoter	This work
M145+ pXZ39	*S. coelicolor* M145 containing pXZ39 that constitutively expresses *eGFP* and *cslZ* from *gapAp* promoter	This work
M145+ pXZ40	*S. coelicolor* M145 containing pXZ40 that constitutively expresses *mCherry* and *cslZ* from *gapAp* promoter	This work

Supplementary Table 2. List of primers used in this study

Primer name	Primer sequence (5' to 3')
GFP-F(NdeI)	GGAATTCCATATGATGGTGAGCAAGGGCGAG
GFP-R(BamHI)	CGCGGATCCTTACTTGTACAGCTCGTCCA
qPCR-cslZ-F	GGATCACCCAGCAGCCCAAG
qPCR-cslZ-R	CCTGGTCCTTCTTGCCCGC
qPCR-cslA-F	CTTCTATCCGATGTCGGCCC
qPCR-cslA-R	GTAGAGCATCAGCCAGACCG
qPCR-hrdB-F	tctctgtcatggcgctcattg
qPCR- hrdB-R	ttccactgagtggccggaatc
qPCR-16S rRNA-F	AGAGTTTGATCCTGGCTCAG
qPCR-16S rRNA-R	CGAACCTCGCAGATGCCTG

Supplementary Table 3. Plasmids used in this work

Plasmids	Description	Reference
pUWL-Cre	Plasmid carrying a Cre-lox recombinase sequence and used to remove apramycin cassette	(161)
pGreen	pIJ8630 containing *eGFP* under control of the constitutive *gapAp* promoter	(25)
pRed	pMS82 containing *mCherry* under control of the constitutive *gapAp* promoter	(25)
pXZ2	pSET152 plasmid containing cslZ expressed from the constitutive gapAp promoter	(14)
pXZ37	pSET152 plasmid containing *eGFP* expressed from the constitutive *gapAp* promoter	This work
pXZ38	pSET152 plasmid containing *mCherry* expressed from the constitutive *gapAp* promoter	This work
pXZ39	pSET152 plasmid containing *eGFP* and *cslZ* expressed from the constitutive *gapAp* promoter	This work
pXZ40	pSET152 plasmid containing *mCherry* and *cslZ* expressed from the constitutive *gapAp* promoter	This work